


RESEARCH ARTICLE

Open Access



# Molecular evolutionary and structural analysis of human *UCHL1* gene demonstrates the relevant role of intragenic epistasis in Parkinson's disease and other neurological disorders

Muhammad Saqib Nawaz<sup>1</sup>, Razia Asghar<sup>1</sup>, Nashaiman Pervaiz<sup>1</sup>, Shahid Ali<sup>1</sup>, Irfan Hussain<sup>1</sup>, Peiqi Xing<sup>2,3</sup>, Yiming Bao<sup>2,3\*</sup> and Amir Ali Abbasi<sup>1\*</sup> 

## Abstract

**Background:** Parkinson's disease (PD) is the second most common neurodegenerative disorder. PD associated human *UCHL1* (Ubiquitin C-terminal hydrolase L1) gene belongs to the family of deubiquitinases and is known to be highly expressed in neurons (1–2% in soluble form). Several functions of *UCHL1* have been proposed including ubiquitin hydrolyze activity, ubiquitin ligase activity and stabilization of the mono-ubiquitin. Mutations in human *UCHL1* gene have been associated with PD and other neurodegenerative disorders. The present study aims to decipher the sequence evolutionary pattern and structural dynamics of *UCHL1*. Furthermore, structural and interactional analysis of *UCHL1* was performed to help elucidate the pathogenesis of PD.

**Results:** The phylogenetic tree topology suggests that the *UCHL1* gene had originated in early gnathostome evolutionary history. Evolutionary rate analysis of orthologous sequences reveals strong purifying selection on *UCHL1*. Comparative structural analysis of *UCHL1* pinpoints an important protein segment spanning amino acid residues 32 to 39 within secretion site with crucial implications in evolution and PD pathogenesis through a well known phenomenon called intragenic epistasis. Identified critical protein segment appears to play an indispensable role in protein stability, proper protein conformation as well as harboring critical interaction sites.

**Conclusions:** Conclusively, the critical protein segment of *UCHL1* identified in the present study not only demonstrates the relevant role of intraprotein conformational epistasis in the pathophysiology of PD but also offers a novel therapeutic target for the disease.

**Keywords:** *UCHL1*, Epistasis, Neurodegenerative diseases, Parkinson's disease, SNCA

\* Correspondence: [baoym@big.ac.cn](mailto:baoym@big.ac.cn); [abbasiam@qau.edu.pk](mailto:abbasiam@qau.edu.pk)

<sup>2</sup>National Genomics Data Center & CAS Key Laboratory of Genome Sciences and Information, Beijing Institute of Genomics, Chinese Academy of Sciences and China National Center for Bioinformatics, Beijing 100101, China

<sup>1</sup>National Center for Bioinformatics, Program of Comparative and Evolutionary Genomics, Faculty of Biological Sciences, Quaid-i-Azam University, Islamabad 45320, Pakistan

Full list of author information is available at the end of the article



© The Author(s). 2020 **Open Access** This article is licensed under a Creative Commons Attribution 4.0 International License, which permits use, sharing, adaptation, distribution and reproduction in any medium or format, as long as you give appropriate credit to the original author(s) and the source, provide a link to the Creative Commons licence, and indicate if changes were made. The images or other third party material in this article are included in the article's Creative Commons licence, unless indicated otherwise in a credit line to the material. If material is not included in the article's Creative Commons licence and your intended use is not permitted by statutory regulation or exceeds the permitted use, you will need to obtain permission directly from the copyright holder. To view a copy of this licence, visit <http://creativecommons.org/licenses/by/4.0/>. The Creative Commons Public Domain Dedication waiver (<http://creativecommons.org/publicdomain/zero/1.0/>) applies to the data made available in this article, unless otherwise stated in a credit line to the data.

## Background

Parkinson's disease (PD) is the second most common neurodegenerative disorder after Alzheimer's disease (AD) and is known to effect normal function of motor neurons [1]. PD prevalence is 1–2% of population above age 65 years and 4–5% above the age of 85 years [2]. There are two major pathological hallmarks of PD diagnosis, selective degeneration of dopaminergic neurons in substantia nigra (it's a basal ganglia structure located in mid-brain that plays a key role in reward, addiction and movement) and the presence of an intracellular protein inclusion, lewy bodies (LBs) and lewy neuritis [2, 3]. PD-associated symptoms include motor features (rigidity, resting tremor, bradykinesia and postural instability) and non-motor features (olfactory dysfunction, autonomic dysfunction, cognitive impairment and psychiatric symptoms) [4]. Since 1997, 27 PD-associated genes have been identified with autosomal dominant (*UCHL1*, *GBA*, *GIGYF2*, *DNAJC13*, *LRRK2*, *TMEM230*, *GCH1*, *EIF4G1*, *SNCA*, *HTRA2*, *RIC3*, *ATXN2*, *VPS35*, *CHCHD2*), autosomal recessive (*PRKN*, *PTRHD1*, *DJ1*, *PLA2G6*, *SPG11*, *FBXO7*, *DNAJC6*, *SYNJ1*, *ATP13A2*, *VPS13C*, *PODXL*, *PINK1*) or an X-linked mode of transmission (*RAB39B*) [5]. *UCHL1* (Ubiquitin C-Terminal Hydrolase 1) is identified as a major causal gene involved in the early-onset of familial and sporadic PD and other neurodegenerative disorders like AD [6, 7] and Huntington's disease [8]. As of now, five missense mutations in *UCHL1* has been associated with PD and other neurological disorders, i.e. E7A [7], S18Y [9], I93M [10], R178Q and A216D [11].

Ubiquitin C-terminal hydrolase L1 (*UCHL1*) is a 24.8 kDa, acidic protein (pI 5.3) [12], consisting of 223 amino acids and encoded by 9 exons with a transcript of 1172 bps in length, and located on human chromosome 4(4p14) [13]. *UCHL1* (PGP 9.5 or PARK5) is the most abundant protein constituting 1–2% of the total brain soluble fraction, which is normally expressed exclusively in neurons and testis and is known to play a key role in ubiquitin turnover through its C-terminal hydrolase activity [3]. However, abnormal expression of *UCHL1* is found in many primary lung tumors, lung tumor cell lines and colorectal cancers [14, 15]. *UCHL1* functions as a de-ubiquitinating or hydrolase enzyme in the ubiquitin-proteasome pathway [11]. Furthermore, it also shows ubiquitin ligase activity for monoubiquitinated  $\alpha$ -synuclein in a cell free system [16]. In addition, *UCHL1* stabilizes the monoubiquitin or free ubiquitin and thus provides the availability of ubiquitin in various other cellular events independently of its enzymatic activity [17]. In the secondary structure comparison, circular dichroism analysis revealed that the mutant version of *UCHL1* (I93M) has decreased level of alpha helix as compared to wild-type *UCHL1*, and therefore has a tendency to

aggregate in neurons [18] and cause autosomal dominant form of PD [10]. Transgenic mouse analysis of mutant version of *UCHL1* (I93M) exhibits the physiological phenotypes related to PD and degeneration of dopaminergic neurons within the age of 20 weeks [19]. Mutant version of *UCHL1* (I93M) also exhibits increased insolubility, aberrant interactions with other proteins (HSP90 & HSC70) in mammalian cells and decreased interaction with monoubiquitin, suggesting that this mutant version (I93M) plays a causative role in familial PD [16]. Furthermore, in vitro analysis of recombinant *UCHL1* (I93M) indicated the decline of 50% hydrolase activity or deubiquitinating activity as compared to the wild type [18, 20] which also contributes to the oxidative modification of *UCHL1* [16, 19]. Intriguingly, subset of mutant versions of *UCHL1* (S18Y) show lower risk of PD due to its reducing ligase activity that leads to reduced level of ubiquitinated alpha-synuclein [21]. However, some studies failed to identify these types of association between mutant version of *UCHL1* (S18Y) and reduced risk of PD [22, 23]. At the molecular level, a missense mutant version of *UCHL1* (E7A) exhibits extensive loss of ubiquitin binding ability thereby leading to completely abolished *UCHL1* hydrolase activity [3, 7]. This loss of function can be rationalized at structural level because glutamic acid (at E7 position of wild type *UCHL1*) is located at ubiquitin binding interface to form electrostatic interactions with ubiquitin residues Arg42 and Arg72 [3]. A recent study analyzed the biochemical impact of the two PD causing *UCHL1* missense mutations suggesting that mutant version of *UCHL1* (R178Q) exhibits a 4-fold increased hydrolase activity as compared to the wild type. This increased enzymatic activity provides a protective effect on cognitive function. Another mutant version of *UCHL1* (A216D) showed insolubility and consequently the complete loss of function [11].

Given the vital role of *UCHL1* in both familial and sporadic PD and other neurological disorders, the present study offers an insight into the evolutionary history of *UCHL1* through evolutionary rate analysis and phylogenetic investigation. Furthermore, the present study provides the comparative analysis of *UCHL1* protein at sequence, structural and interaction level. Comparative sequence and structural information inferred the strong epistasis influence of evolutionary and disease causing amino-acid substitutions on a small protein segment (amino acids 32 to 39) within N-terminal C-12 peptidase domain of *UCHL1*. Functional implications of identified critical protein segment were further evaluated through interaction analysis of *UCHL1* with its interacting partners SNCA (PARK1) and PARKIN (PARK2).

**Results**

**Phylogenetic analysis**

In order to analyze the evolutionary history of PD-associated *UCHL1* gene, Neighbor-joining (NJ) and Maximum likelihood (ML) trees were constructed. The phylogenetic tree topology suggests that *UCHL1* is a gnathostomata (jawed vertebrate) specific gene and present in tetrapods, bony fishes and in cartilaginous fishes. Bidirectional BLAST based similarity searches did not identify orthologous counter part of this gene in any of the non-gnathostomata vertebrates or invertebrate animals analyzed in the present study. Furthermore, similarity searches failed to detect any paralogous copy of

*UCHL1* in any of the gnathostomata clades analyzed. (Fig. 1 and Additional file 1: Figure S1).

**Evolutionary rate analysis of *UCHL1* gene in sarcopterygians**

In order to analyze evolutionary rate differences of the *UCHL1* gene within different groups of sarcopterygians lineage, key animals were selected from four groups like hominoids (human, chimpanzee, gorilla and orangutan), non-hominoids (macaque, squirrel monkey, marmoset and Otolemur), non-primate placental mammals (cow, cat, elephant and mouse) and non-mammalian tetrapods (chicken, zebra finch, turtle and coelacanth). The rationale

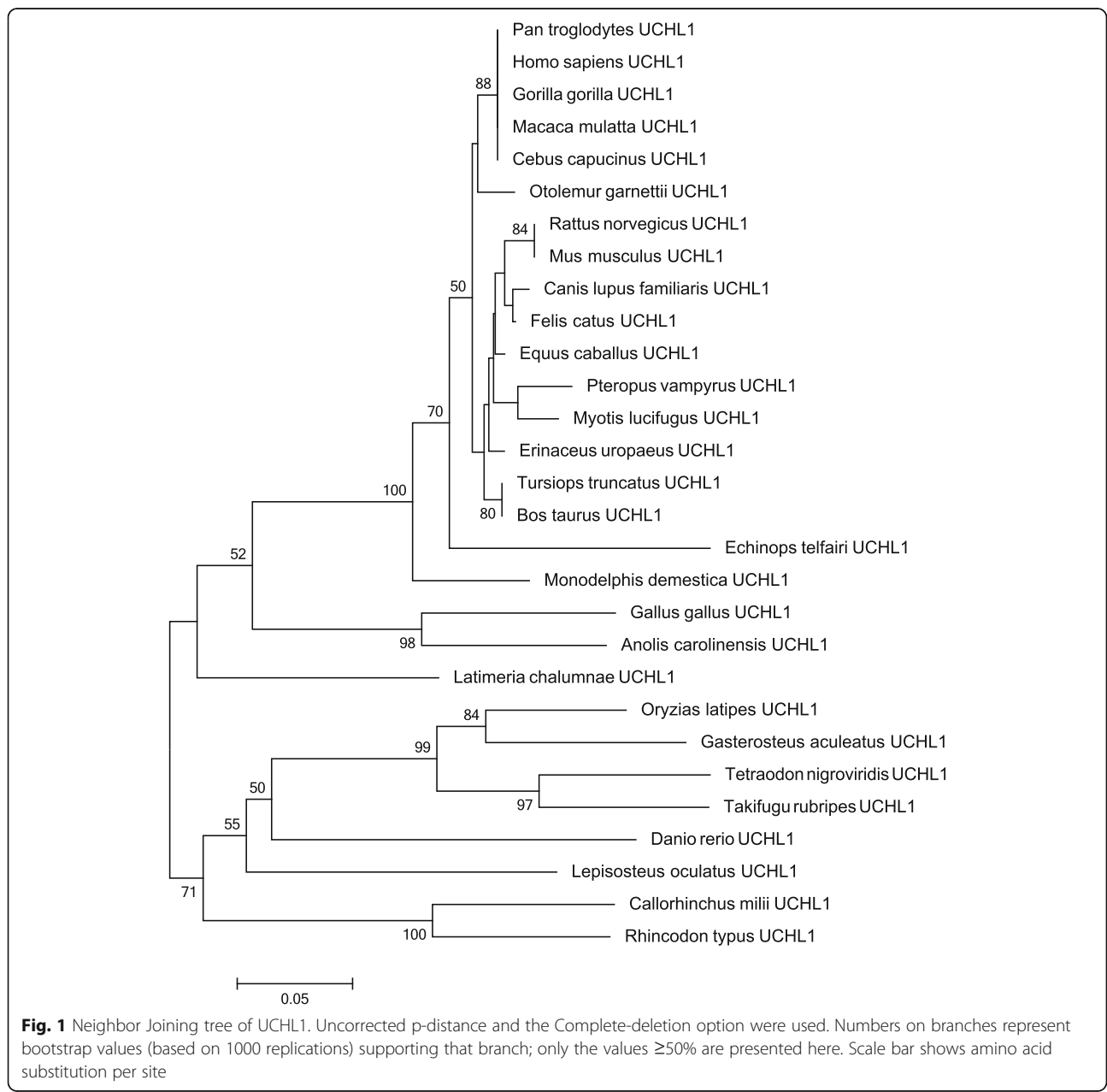


**Fig. 1** Neighbor Joining tree of *UCHL1*. Uncorrected p-distance and the Complete-deletion option were used. Numbers on branches represent bootstrap values (based on 1000 replications) supporting that branch; only the values  $\geq 50\%$  are presented here. Scale bar shows amino acid substitution per site

behind choosing only sarcopterygians for evolutionary rate analysis is that animals of this lineage are known to be more closely related or show more homology to humans as compare to teleost and cartilaginous fishes [24]. To evaluate the selection constraints on selected subgroups of animals, the rates of non-synonymous ( $K_a/dN$ ) and synonymous ( $K_s/dS$ ) substitutions were estimated and their difference was calculated using z-test [25]. In general,  $K_a$  value lower than  $K_s$  ( $K_a < K_s$ ) suggests negative selection, i.e. non silent substitutions have been purged by natural selection, whereas the inverse scenario ( $K_a > K_s$ ) implies positive selection, i.e. advantageous mutations have accumulated during the course of evolution. However, the evidence for positive or negative selection requires the values to be significantly different from each other [26, 27].

The  $K_a$ - $K_s$  ( $dN$ - $dS$ ) difference was  $-2.747$  ( $P = 0.007$ ) for hominoids,  $-6.501$  ( $P = 0$ ) for non-hominoids,  $-8.945$  ( $P = 0$ ) for non-primate placental mammals,  $-8.199$  ( $P = 0$ ) for non-mammalian tetrapods (Additional file 2: Table S1). These data suggest that during the course of sarcopterygians evolution, *UCHL1* has deviated significantly from neutrality and evolved under strong negative selection (Additional file 2: Table S1).

#### Domain organization of UCHL1 protein

In order to investigate the comparative domain organization of UCHL1, complete domain, motifs and sub-motifs were identified through extensive literature survey as well as using different tools/databases [28, 29]. UCHL1 contains a single domain that spans a large portion of protein (amino-acids 3 to 206), which is named as C-12 peptidase domain. It regulates substrate access to the catalytic site [30]. The C-12 peptidase domain comprises of cysteine active-site (84–100), N-myristoylation sites (87–92, 94–99), Casein Kinase II Phosphorylation sites (119–122, 125–128, 188–191, 205–208), Protein kinase C phosphorylation sites (76–78, 121–123, 205–207) [29] and unconventional pathway secretion site of UCHL1 (32–39) [31]. The farnesylation-site (220–223) [32] resides outside of the C-12 domain at the C-terminal of UCHL1 (Fig. 2a). These domains, motifs and sub-motifs are comparatively mapped on orthologs from major representative species of sarcopterygians, like primate (human), non-primate placental mammals (mouse and cat), non-mammalian tetrapods (chicken) and lobe-finned fish (coelacanth) (Fig. 2a).

Annotation and comparative analyses at sequence level revealed that the C-12 peptidase domain and its major motifs like the unconventional pathway secretion site of UCHL1 (32–39) [31], cysteine active-site (84–100) and N-myristoylation sites (87–92, 94–99) are highly conserved within selected subgroup of sarcopterygians animals (Fig. 2a). Three protein kinase C (PKC) phosphorylation sites (76–78, 121–123, 205–207) and four casein kinase II (CK2) phosphorylation

sites (119–122, 125–128, 188–191, 205–208) are also found to be highly conserved in mammals (human, mouse and cat), whereas in chicken a PKC phosphorylation site appears to have been translocated from C-terminal to N-terminal of UCHL1 and an additional PKC phosphorylation site (198–200) is detected. Furthermore, both in chicken and coelacanth one N-myristoylation site appears to have been translocated from C-terminal to N-terminal of UCHL1 (at position 21–26). In both chicken and coelacanth, a CK2 phosphorylation site (119–122) is not detected and some translocations of PKC phosphorylation sites are also observed (Fig. 2a).

By employing ancestral reconstruction technique five mammalian specific evolutionary substitutions were identified and mapped on human UCHL1 protein. One of them occurred at the root of primate's lineage, three at the root of simian's lineage and one specifically in ape's history (Fig. 2a and Table 1). Analysis of physicochemical properties of these five mammalian specific amino acid substitutions suggests that all of them are of radical type (Table 1). All these evolutionary substitutions are localized within the C-12 peptidase domain (Fig. 2a). In addition, previously reported 5 PD and other neurological disorders associated missense mutations (E7A, S18Y, I93M, R178Q and A216D) are also localized to the C-12 peptidase domain except A216D which resides at the C-terminal of human UCHL1. These data reveal that highly conserved C-12 peptidase domain has a significant role not only in the evolutionary/functional perspective but also in disease pathogenesis. The SLAC-window analysis identified 73 negatively constrained sites within the C-12 peptidase domain of UCHL1 (Fig. 2b and Additional file 2: Table S2).

#### Protein structural evolution of UCHL1

Comparative protein structure modeling was performed to inspect how negative selection is performing its role in defining the spatial constraints on ancestral UCHL1 proteins. Ancestral protein structures (mammals, primates, simians and apes) obtained from the MODELLER program were superimposed at an appropriate evolutionary scope, i.e. mammals-primates ancestors, primates-simians ancestors and simians-apes/human ancestors (Fig. 3). Protein structural deviations were examined with the help of Chimera and root mean square deviation (RMSD) values (Fig. 3 and Table 2). Comparative structural investigations revealed very notable aspects of UCHL1 evolution that were not anticipated by comparative analysis at sequence level alone. It appears that during the course of mammalian evolution the UCHL1 has undergone strong intragenic epistatic interactions to acquire its favorable protein conformation. Aforementioned superimposed protein models revealed a common deviated region composed of amino acids 32 to 39 within the secretion site at the N-terminal of C-12 peptidase domain (Table 2). These structural deviations were

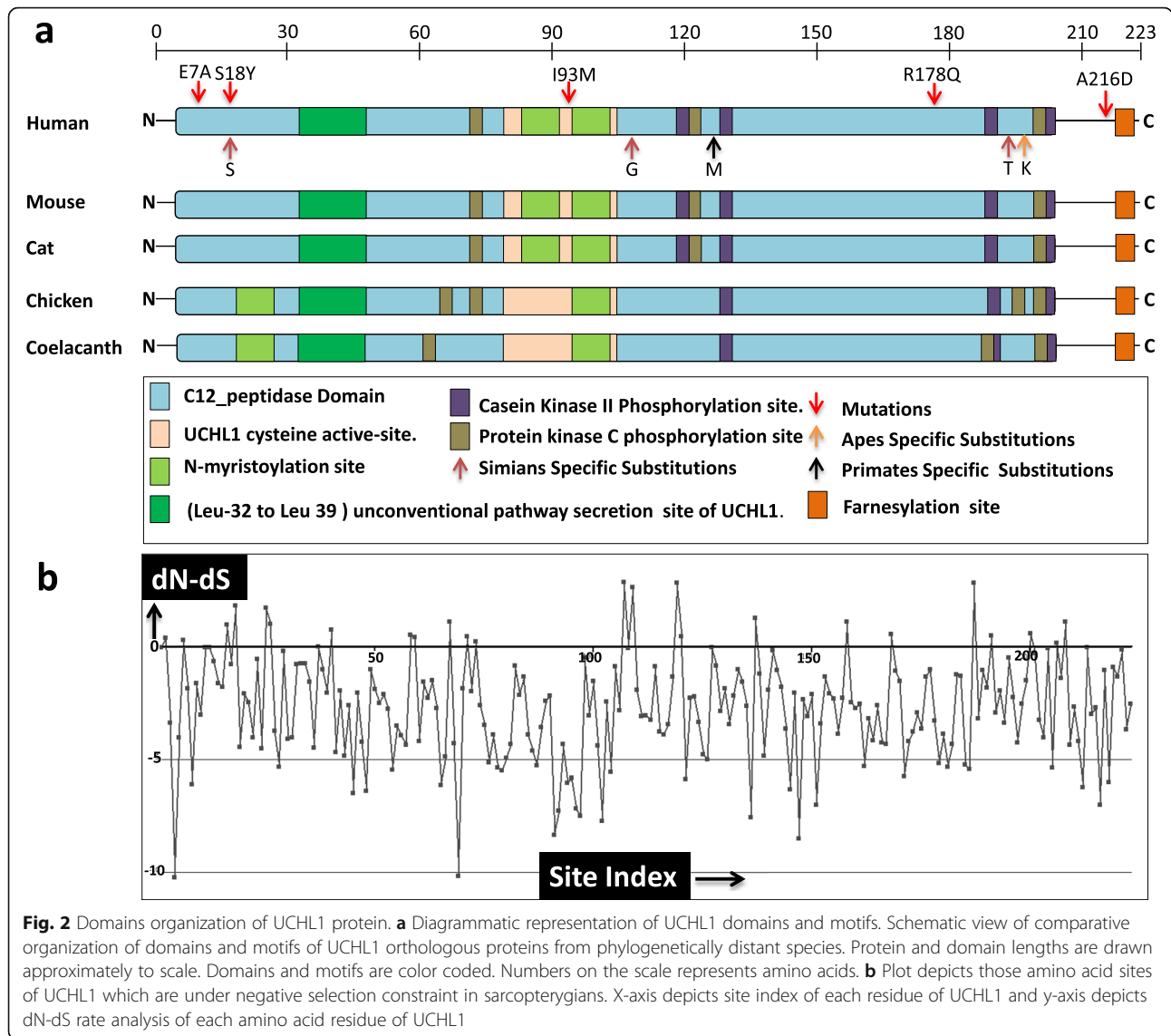


**Table 1** Amino-acid replacements in UCHL1 during primate history

| Position | Mammals ancestral residues | Replacement in ancestor of primates | Replacement in ancestor of simians | Replacement in ancestor of apes. | Neutral/Radical | Impact on protein stability | Location motif/domain |
|----------|----------------------------|-------------------------------------|------------------------------------|----------------------------------|-----------------|-----------------------------|-----------------------|
| 18       | A                          |                                     | S                                  |                                  | Radical (+ 1)   | Decreased (-0.85)           | Peptidase C12 domain  |
| 107      | E                          |                                     | G                                  |                                  | Radical (-2)    | Decreased (-1.79)           | Peptidase C12 domain  |
| 124      | L                          | M                                   |                                    |                                  | Radical (+ 2)   | Decreased (-0.74)           | Peptidase C12 domain  |
| 192      | S                          |                                     | T                                  |                                  | Radical (+ 1)   | Decreased (-0.79)           | Peptidase C12 domain  |
| 195      | Q                          |                                     |                                    | K                                | Radical (+ 1)   | Decreased (-1.45)           | Peptidase C12 domain  |

After the divergence from mammal's ancestor, one amino-acid change occurred in the root of primates, three replacements occurred specifically in the ancestor of Simians lineage whereas one replacement occurred in apes history. The 6th column depicts the putative physicochemical impact of each replacement on protein/structure function. The number within brackets is the log odds associated with changing the amino acids. Positive numbers imply a preferred change, zero implies a neutral change and negative numbers imply an un-preferred change. The 7th column depicts the putative impact of each replacement on stability of protein. The numbers within brackets are the confidence scores (i.e. from -1 to 1) associated with the impact on stability of protein structure by changing the amino acids. Positive numbers imply an increase in stability of protein structure. The bigger the score, the more confident the prediction is. Conversely, negative numbers imply a decrease in the stability of protein structure



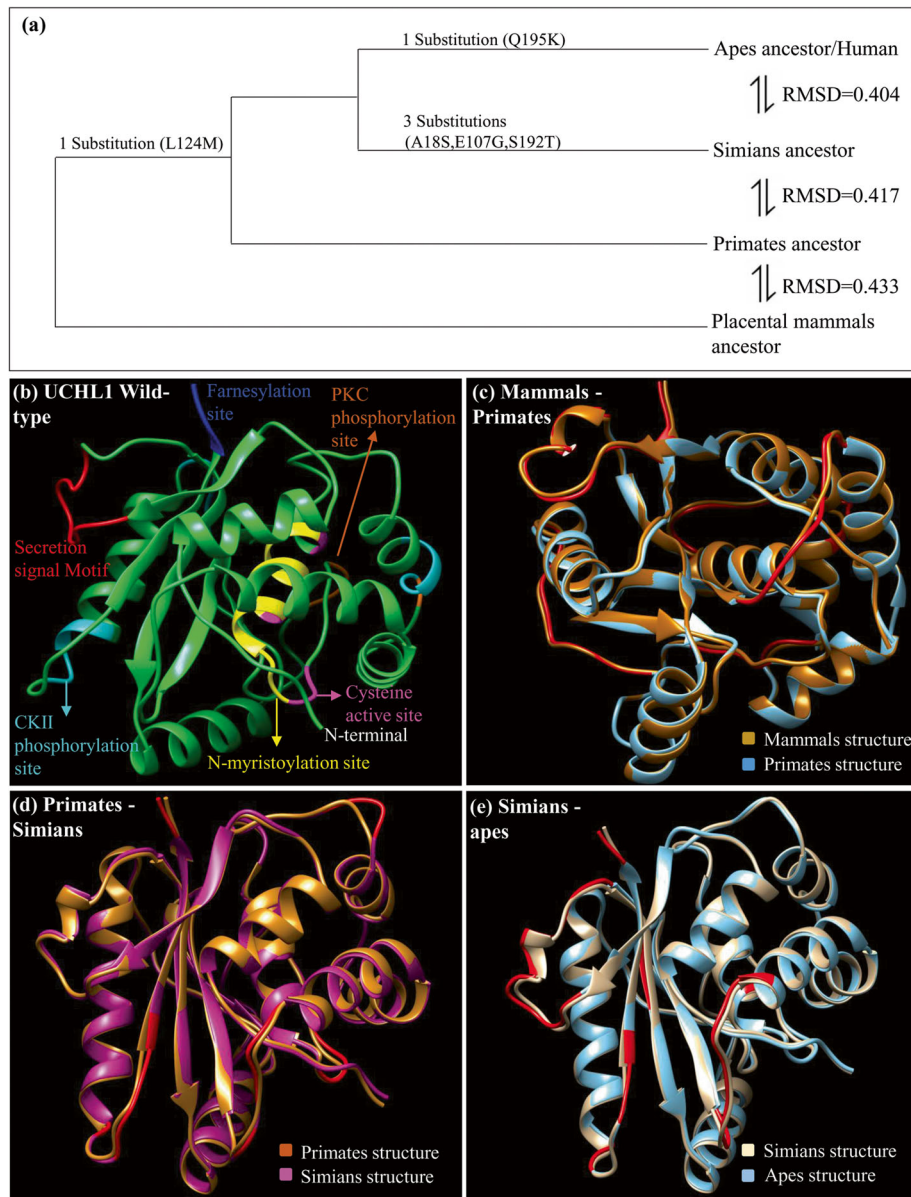


**Fig. 3** Structural evolution of UCHL1 protein. **a** Structural divergence of human UCHL1 after the split from placental mammals common ancestor. One primate specific substitution has occurred which is retained in simians and apes after they diverged from the placental mammalian ancestor. Whereas, three substitutions have occurred specifically at the root of simians lineage and one apes specific substitution is also detected. Structural deviations among ancestors are examined by RMSD values. **b** Annotated structure of wild type UCHL1. **c** Superimposed placental mammals ancestor and primates ancestor structures. **d** Superimposed primates ancestor and simians ancestor structures. **e** Superimposed simians ancestor and apes ancestor structures. Deviated residues in terms of backbone torsion angles ( $\Phi^\circ$ ,  $\Psi^\circ$ ) are represented in red color and all superimposed structures are color coded

also measured with the help of backbone torsions quantification which also suggests that protein segment composing of amino acids 32 to 39 has evolved during mammalian history through a well-known phenomenon called intragenic epistasis [33]. It appears that during the course of evolution, mammalian UCHL1 has incorporated destabilizing substitutions to obtain its intrinsic disordered conformation through radical structural shifts in this

identified critical region. This critical region (amino acids 32–39) is recognised as crucial for proper conformation of not only unconventional pathway secretion site of UCHL1 protein but also for the entire C-12 peptidase domain.

Interestingly, all the previously reported human specific missense mutations associated with familial and sporadic PD and other neurological disorders are confined to the C-12 peptidase domain except A216D. To investigate the

**Table 2** Structural comparisons of predicted ancestral UCHL1 proteins

| Comparison between lineages   | Major change in backbone torsion angles   | Major shifts in region   | Critical region                |
|-------------------------------|---|--|--------------------------------|
| Mammals ↔ Primates ancestor   | Leu32-Gly40<br>Pro43-Ala46, Lys71-Ser76, Gln103-Gly111,<br>Asn136,<br>Glu149-Arg153,<br>Gly210-Valn212        | Secretion Signal motif<br>C12- Peptidase domain<br><br>C-terminal region | 32–39 (Secretion Signal Motif) |
| Primates ↔ Simians ancestor   | Ser41-Val43, Ala48-Leu50, Gln84-Gly87,<br>Glu109-Gly111,<br>Gly150-Asp156,<br>Gly210-Ser215,<br>Ala222-Ala223 | C12-peptidase Domain<br><br>C-Terminal region<br>Farnesylation site      | —                              |
| Simians ↔ Apes/human ancestor | Val31-Gly39<br>Ser41-Val42, Glu208-Ser215, Glu149-Cys152,<br>Val154-Asn159,<br>Glu203                         | Secretion Signal motif<br>C12- Peptidase domain<br><br>C Terminal region | 32–39 (Secretion Signal Motif) |

This table shows the effect of lineage specific substitutions on the backbone torsion angles of ancestral UCHL1 protein structures through comparisons among lineages given in first column

impact of these previously reported missense mutations at protein structure level, all disease causing mutant structures (previously reported missense mutations) of UCHL1 were predicted through MODELLER and superimposed on 2ETL (the wild type version of UCHL1) (Fig. 4). In addition, wild-type protein structure of UCHL1 and disease causing mutant versions were also predicted through I-TASSER server (Additional file 1: Figure S2 and Additional file 2: Table S3) and Robetta server (Additional file 1: Figure S3 and Additional file 2: Table S4). I-TASSER and Robetta predicted wild-type and mutant protein structures of UCHL1 were also superimposed (Additional file 1: Fig. S2, Fig. S3 and Additional file 2: Table S3, Table S4). Structural deviations between wild type and mutant versions were evaluated using RMSD values. Intriguingly, even though the disease causing mutations are spread across UCHL1, all of them appear to impact the structure of common protein region spanning amino acids 32–39 (secretion site of UCHL1). In addition another protein region (amino acids 222–223) within farnesylation site is deviated in all disease causing mutant models except for E7A (Fig. 4 and Table 3; Additional file 1: Figure S2 and Figure S3; Additional file 2: Table S3 and Table S4). Therefore, UCHL1 protein segment spanning amino acids 32–39 is considered as critical not only in evolutionary perspective but also in disease pathogenesis.

#### Protein-protein interaction analysis of UCHL1

In order to further investigate the significance of identified critical protein segment, we performed the interaction analysis of human UCHL1 with its biochemically and genetically verified interacting partner proteins. The identification of pathogenic mutations in the three human genes, i.e. SNCA (PARK1), PARKIN (PARK2), and UCHL1 (PARK5) has elucidated the ubiquitin proteasome system (UPS) and its potential role as a causal pathway in PD [34]. Furthermore, the STRING database reveals

information that SNCA and PARKIN are the interacting partners of UCHL1 [35]. For protein-protein interaction analyses the domain architecture of SNCA and PARKIN is also annotated (Fig. 5). Human SNCA protein comprises of 140 amino acids and contains three major domains named as A2 lipid binding alpha helix domain, NAC domain and C-terminal acidic domain [2]. Furthermore, PARKIN comprises of 465 amino acids and contains 5 domains named as Ubl domain, RING0, RING1, in-between RING (IBR) domain and RING2 domain [36].

Interaction analysis between UCHL1 and SNCA depicts only five interacting residues that involves the C-12 peptidase domain of UCHL1 and the NAC domain of SNCA (Fig. 5 and Additional file 2: Table S5). Interaction analysis of five human disease causing mutant versions of UCHL1 with SNCA revealed altered interaction patterns, although some of the wild type interactions are also retained (Additional file 1: Fig. S4 and Additional file 2: Table S6). These data signifies that UCHL1 and SNCA not only interact in normal individuals but also in PD patients with altered interaction pattern (Fig. 5; Additional file 1: Figure S4 and Additional file 2: Table S6).

Intriguingly, in UCHL1 (R178Q)-SNCA docked complex, two altered interactions were found within the identified critical region (amino acids 32–39 within secretion site) of UCHL1, which could potentially affect the normal secretion of UCHL1 to neurons and thus could contribute to disease pathogenesis (Additional file 1: Figure S4 and Additional file 2: Table S6).

Interaction analysis of UCHL1 with PARKIN showed 15 interacting residues involving RING1 and IBR domains of PARKIN and C-12 peptidase domain of UCHL1 (Fig. 5 and Additional file 2: Table S5).

#### Discussion

Advent of high throughput annotation of genomes and broadened availability of genomic sequence data

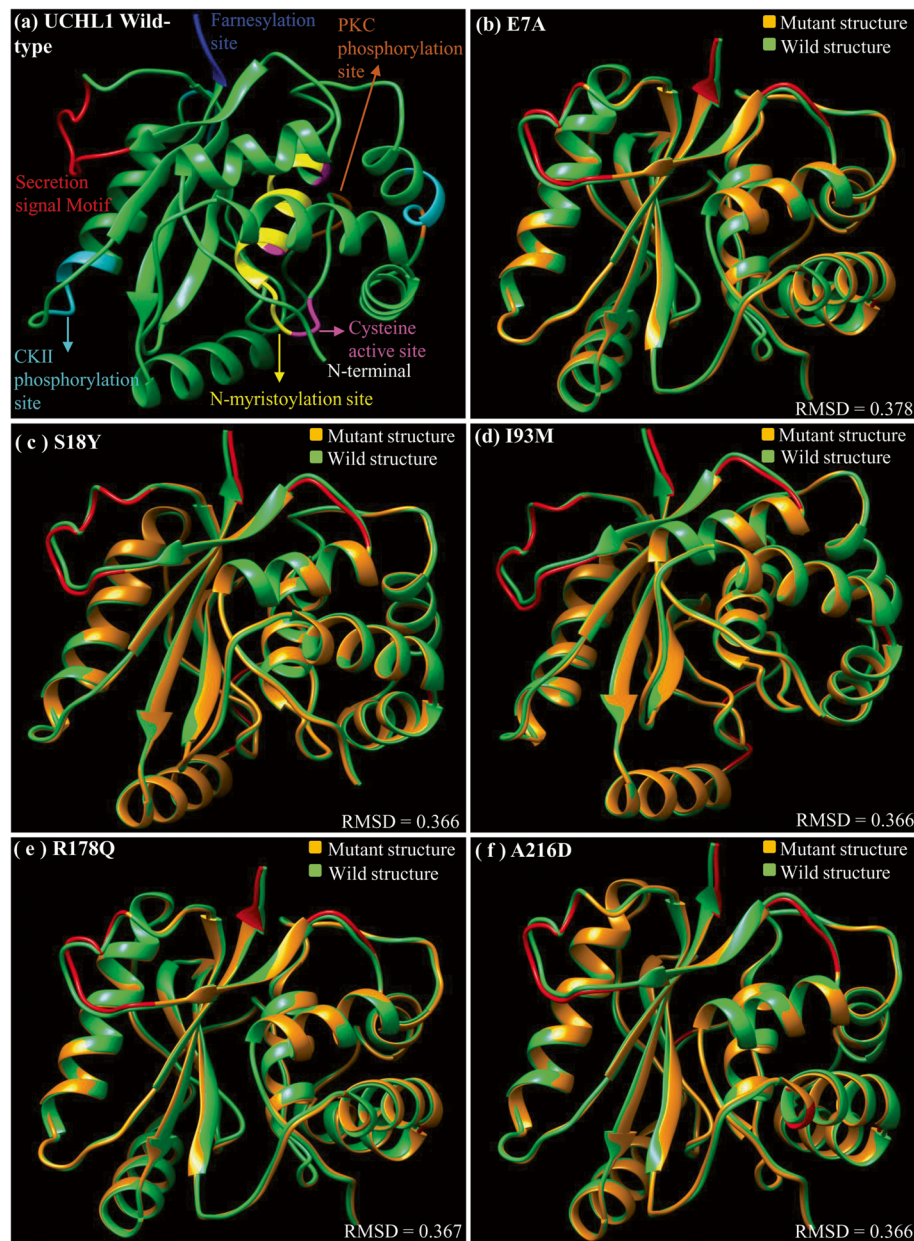


**Fig. 4** Protein structural deviations in PD associated mutant versions of UCHL1. Major structural shifts caused by disease associated missense mutations of UCHL1 are observed in the secretion signal and farnesylation motifs present in the N-terminal and C-terminal respectively. Deviated residues are labeled in red. **a** Structure of wild type UCHL1 in which all domains and motifs are color coded. **b** Structural superimposition of wild type (green) and mutated model E7A (coral peach). **c** Structural comparison between wild type UCHL1 (green) and mutated model S18Y (coral peach). **d** Structural deviations among wild type UCHL1 (green) and mutated model I93M (coral peach). **e** Structural comparison between UCHL1 (green) and mutated model R178Q (coral peach). **f** Structural superimposition of the wild type (green) and mutated model A216D (coral peach)

permitted to investigate the evolutionary history of genes of interest and link it to human disease associated phenotypic traits [26]. Ubiquitin proteasome pathway (UPP) is the most important molecular mechanism that participates in neurodegenerative diseases such as PD and AD. The major pathological hallmarks of these two important neurodegenerative disorders are characterized by the accumulation of abnormal

protein aggregates (AD: Extracellular A $\beta$  amyloid plaque; PD: Intracellular  $\alpha$ -synuclein in the Lewy body) within the neurons [37, 38]. UPP is the major mechanism which serves to recognize the damaged or misfolded proteins and transport them to the proteasome for degradation. By this way UPP maintains the normal concentration of proteins in the neurons and thus prevent neurodegeneration [39, 40]. UPP



**Table 3** Structural comparisons of disease causing mutant versions of UCHL1 protein

| Mutations | Major changes in residue number | Major shifts in region   | Critical region                 |
|-----------|---------------------------------|--------------------------|---------------------------------|
| Ile93Met  | 23–24                           | C12-peptidase Domain     | 32–39 (Secretion, Signal Motif) |
|           | 32–38                           | Secretion signal Motif   |                                 |
|           | 45,74–75                        |                          |                                 |
|           | 136,148                         |                          |                                 |
|           | 222–223                         | Farnesylation site       |                                 |
| Glu7Ala   | 22–25                           | C12-peptidase Domain     | 32–39 (Secretion, Signal Motif) |
|           | 31–38                           | Secretion signal Motif   |                                 |
|           | 45,74–75                        |                          |                                 |
|           | 111–112                         |                          |                                 |
|           | 190–191,136                     | CK2 Phosphorylation site |                                 |
| Ser18Tyr  | 23–25,                          | C12 peptidase Domain     | 32–39 (Secretion, Signal Motif) |
|           | 31–38,                          | Secretion signal Motif   |                                 |
|           | 45,74–75                        |                          |                                 |
|           | 111–112                         |                          |                                 |
|           | 150–152                         |                          |                                 |
|           | 148,136                         |                          |                                 |
|           | 222–223                         | Farnesylation site       |                                 |
| Arg178Gln | 23–24                           | C12-peptidase Domain     | 32–39 (Secretion, Signal Motif) |
|           | 32–39                           | Secretion signal Motif   |                                 |
|           | 136,74                          |                          |                                 |
|           | 221–223                         | Farnesylation site       |                                 |
| Ala216Asp | 23–24                           | C12-peptidase Domain     | —                               |
|           | 74–75                           |                          |                                 |
|           | 136,148                         |                          |                                 |
|           | 222–223                         | Farnesylation site       |                                 |

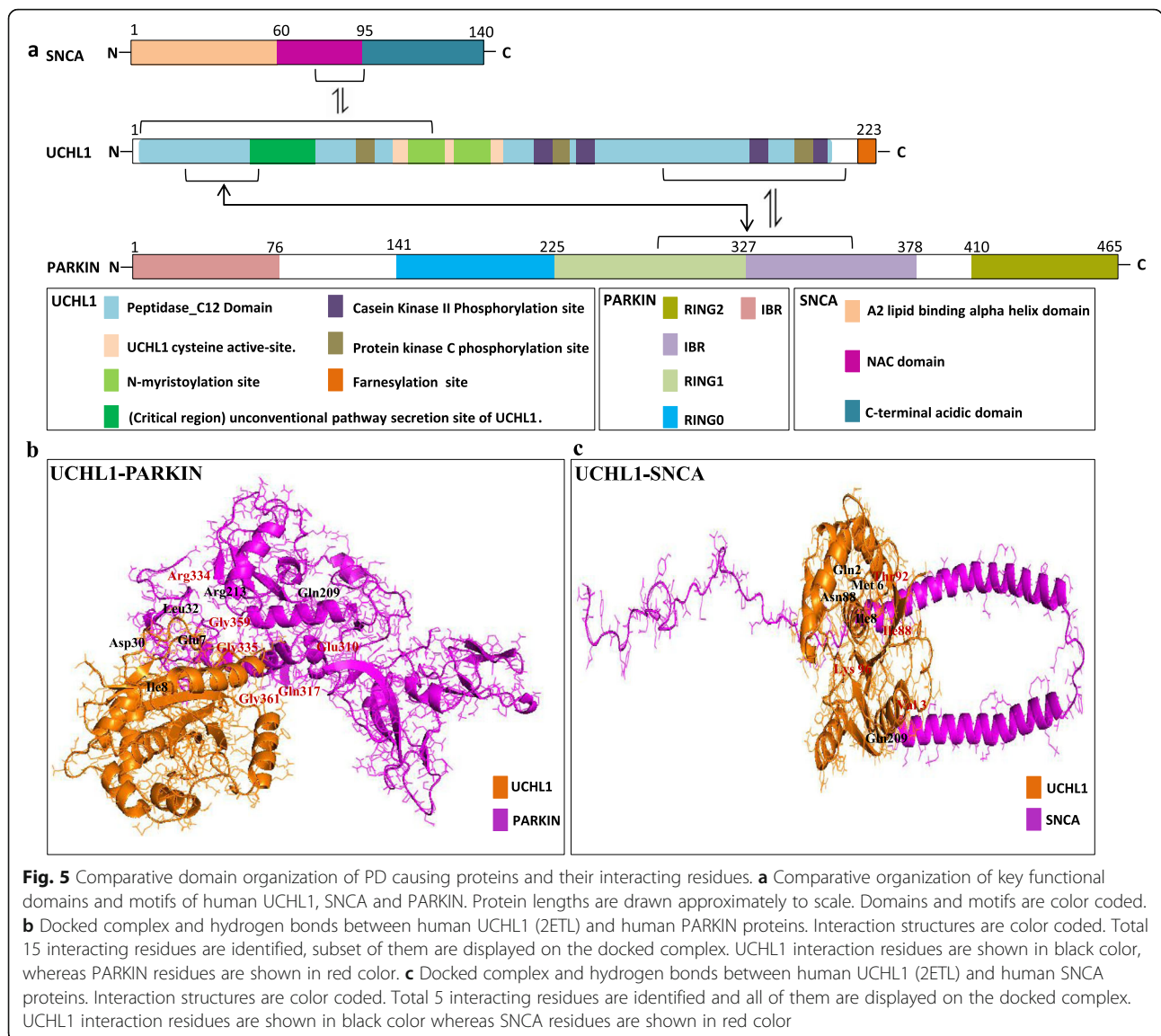
This table shows the impact of PD (Parkinson's disease) and other neurological disorders causing missense mutations on backbone torsion angles of human UCHL1 protein. In the first column, amino acid residue on the left indicates the wild-type residue, whereas the residue on the right is mutated version; number indicates the amino acid position. The second column specifies the positions at which major structural deviations are observed. The third column depicts the deviated region. The fourth column depicts deviated residues shared among all mutant structures of UCHL1 protein

contains several components that include 26S proteasome, ubiquitin, ubiquitin activating enzyme E1, ubiquitin conjugating enzyme E2 and ubiquitin ligating enzyme (E3). The *UCHL1* gene product is a key component of UPP and functions as deubiquitinating enzymes to remove ubiquitin from proteins and it also stabilizes the monomer ubiquitin in cell free system [11, 41]. Furthermore, UCHL1 is also known to facilitate E3 ligase in UPP [42–44]. The *UCHL1* gene product has also been implicated in processes like apoptosis, protection against oxidative stress [45], long-term protonation [20] and chaperone-mediated autophagy [16]. However, the role of UCHL1 in these processes have not yet been fully understood [32].

UCHL1 consists of 223 amino acids with a single domain. It belongs to a  $\alpha/\beta$  fold protein family with six  $\beta$ -strands inside the hydrophobic core, which is surrounded by seven  $\alpha$ -helices [12]. Five missense mutations in human *UCHL1* gene have so far been associated with autosomal

dominant PD, recessive hereditary spastic paraplegia (SPG79) and early onset of progressive neurodegeneration. The present study is an attempt to investigate sequence and structural bases of UCHL1 evolution within the sarcopterygians lineage. Furthermore, this study elucidates protein structural and interactional basis of UCHL1-associated PD pathogenesis.

The ML and NJ based phylogenetic tree topologies of the *UCHL1* gene supported by high bootstrap values revealed that it is gnathostomata (jawed-vertebrate) specific gene and present in tetrapods, bony fishes and in cartilaginous fishes. Bidirectional BLAST based similarity searches did not identify orthologous counter part of this gene in any of the non-gnathostomata vertebrates and invertebrate animals analyzed. Furthermore, similarity searches failed to detect any paralogous copy of *UCHL1* in any of the gnathostomata (jawed-vertebrate) clades analyzed. Based on these phylogenetic data, it is speculated that human *UCHL1* might have



originated at the root of jawed vertebrates (Fig. 1 and Additional file 1: Figure S1). These observations prompted us to evaluate the selection constraints on this gene within different selected subgroups of animals in sarcopterygians lineage. For this purpose, the rates of non-synonymous ( $K_a/dN$ ) and synonymous ( $K_s/dS$ ) substitutions were estimated within each selected subgroups of animals and their difference was calculated using z-test. These statistical estimations corroborate well with the speculation that *UCHL1* has evolved under strong purifying selection throughout the sarcopterygians history, which might have discouraged any functional modification to happen through gene duplications (Additional file 2: Table S1).

The C-12 peptidase domain is a major domain that spans the large portion of UCHL1 starting from residue 3 (at N-terminal) and ending at 206 residues (at C-

terminal). Comparative domain organization data suggests that the C-12 domain and its motifs/sub-motifs are similarly present in all of the animals analyzed with no major variations in protein primary organization. In addition to C12 peptidase domain, extreme N-terminal and C-terminal sites also appear to be highly preserved among all the analyzed sarcopterygian animals (Fig. 2). Intriguingly, conserved domain/motif organization of UCHL1 among distantly related orthologs corroborates well with the signal of strong purifying selection identified through z-statistics and with previously reported functional data on human UCHL1. For instance, a recent study suggests that removal of only eleven residues from the N-terminal of UCHL1 is sufficient for the protein to loss affinity for ubiquitin or lack of deubiquitinating activity and ultimately leads to formation of insoluble aggregates [46, 47]. Minor truncation at N- or C-

terminus of UCHL1 are reported to denature the protein, therefore renders it functionless [48]. In vitro mutagenic and *in-silico* simulation studies revealed that removal of few amino acids either from the C-terminal or from the N-terminal of UCHL1 can destabilize its three dimensional structure, resulting in unfolding or loss of solubility consistent with protein aggregation [46, 48, 49].

Comparative structural analyses were performed to inspect how negative selection is playing its role in defining the spatial constraints on ancestral UCHL1 at structural level (Fig. 3 and Table 2). The comparative structural analysis of predicted ancestral proteins of UCHL1 (mammals ancestor, primates ancestor, simians ancestor and apes/human ancestor) showed multiple deviated regions in each of the predicted ancestral UCHL1. Comparative analysis of ancestral predicted structural data revealed a common deviated region comprises of amino acids 32 to 39 (Fig. 3). This particular protein segment appears to have experienced structural shifts repeatedly during the course of mammalian evolution through strong intragenic epistatic interactions within UCHL1. Furthermore, the protein structural impacts of five identified lineage specific substitutions suggest that UCHL1 has undergone structural destabilization during the course of mammalian history (Table 1). This structural destabilization can best be explained by speculating that during the course of mammal's evolution UCHL1 has acquired the ability to attain favorable conformation upon binding to its targets (Table 1).

Furthermore, we also performed comparative structural analysis of previously reported PD and other neurological disorders causing missense mutations of UCHL1 (between wild type and all five PD and other neurological disorders causing mutant versions). This comparative structural analysis (predicted through Modeller, I-TASSER and Robetta) revealed multiple distinct deviated regions in each comparison as well as a commonly deviated segment comprising of amino acids 32 to 39 within the secretion site at N-terminal of the C-12 peptidase domain (Fig. 4 and Table 3; Additional file 1: Figure S2 and Figure S3; Additional file 2: Table S3 and Table S4). Interestingly, this commonly deviated region (32 to 39) in disease causing variants of UCHL1 also appears to have evolved structurally during mammalian evolution (described in preceding sections). Therefore, the protein segment 32–39 of UCHL1 is both important and indispensable in evolution and PD pathogenesis through intraprotein conformational epistasis [33]. The functional significance of this critical region is supported by previously reported data which suggest that the substitution of the leucine within this region (Leu-32 to Leu-39) leads to reduced secretion of

UCHL1 in cytoplasm of neuronal cells and consequently causing PD phenotype [31]. In addition, the comparative analysis of human UCHL1 structure with all five PD-causing mutant versions (except E7A) revealed another commonly deviated region at C-terminal comprises of protein segment 220–223 within farnesylation site (Fig. 4 and Table 3; Additional file 1: Figure S2 and Figure S3; Additional file 2: Table S3 and Table S4). Functional significance of this second commonly deviated region corroborate well with previously reported data which suggest that the loss of just four amino acids from the C-terminal of UCHL1 is sufficient to induce protein aggregation and consequently neuronal cell death [32, 49]. Taken together, critical regions of UCHL1 identified in the present study (amino acids 32–39 & amino acids 220–223) are important for maintaining normal neuronal physiology and any conformational changes in either of these protein regions could lead to PD disease.

The interaction analysis of UCHL1 with its major interacting partner's, i.e. SNCA and PARKIN further highlights the structural, functional and disease significance of identified critical regions (amino acids 32–39). For instance, the protein-protein interaction analysis revealed that the C-12 peptidase domain of UCHL1 interacts with the NAC domain of SNCA, and the RING1 and IBR domains of PARKIN (Fig. 5). Interestingly, both SNCA and PARKIN appears to interact physically with the identified critical region (amino acids 32–39) of UCHL1 (Fig. 5 and Additional file 2: Table S5). In addition, interaction analysis of five human disease causing mutant versions of UCHL1 with SNCA revealed altered interaction pattern, although some of the wild type interactions are also retained. For instance, docked complex of wild type UCHL1 with disease-causing mutant version of SNCA (A30P) revealed no altered interactions (same as the wild type interaction of UCHL1-SNCA complex) (Additional file 1: Figure S5 and Additional file 2: Table S6). In contrast, docked complex of wild type UCHL1 with another disease-causing mutant version of SNCA (A53T) revealed altered interaction pattern (Additional file 1: Figure S5 and Additional file 2: Table S6). These interaction data corroborate well with previously reported biochemical data which suggests that the A53T mutant version of SNCA impacts the normal secretion of UCHL1 in neuronal cytoplasm [31]. Based on these interaction analyses, it is speculated that UCHL1 and SNCA interact physically, not only in normal individuals but also in PD patients with altered interaction pattern. (Fig. 5; Additional file 1: Figure S4 and Additional file 2: Table S6).

## Conclusion

Human UCHL1 is known to play an important role in ubiquitin stability within neurons which is critical for

ubiquitin–proteasome system and neuronal survival. Mutations in the human *UCHL1* gene have been associated with various neurodegenerative disorders like PD, recessive hereditary spastic paraplegia (SPG79), AD and Huntington's disease. Considering the indispensable role of the *UCHL1* gene product in neuronal physiology and pathophysiology, the current study investigates the sequence evolutionary pattern and structural dynamics of *UCHL1*. Phylogenetic data suggest the ancient origin of *UCHL1* at the root of gnathostomes (jawed vertebrate) history. Furthermore, molecular sequence evolutionary analysis reveals that *UCHL1* has remained under strong functional constraints throughout the gnathostomes history which might have discouraged the duplication of this gene in any of the animal lineage analyzed in the present study. Comparative structural analysis of *UCHL1* pinpointed a critical protein segment (amino acids 32 to 39 within the secretion site) with crucial implications in evolution and PD pathogenesis through a well known phenomenon of intraprotein conformational epistasis. This critical protein segment of *UCHL1* can be targeted for drug designing and investigation for the treatment of PD in future.

## Methods

### Sequence acquisition

The putative orthologous protein sequences of human *UCHL1* were retrieved from protein databases accessible at Ensemble [50] and National Center for Biotechnology Information [51] by using BLAST p bidirectional best hit approach [52]. Further confirmation of the common ancestry of the putative orthologs was obtained by clustering homologous proteins within phylogenetic trees [53, 54]. Sequences whose position within a tree is in sharp conflict with the uncontested animal phylogeny are excluded from the analysis. All protein sequences used in this study are provided in Additional file 3.

List of species selected for sequence analysis of *UCHL1* is *Homo sapiens* (Human), *Pan troglodytes* (Chimpanzee), *Gorilla gorilla* (Gorilla), *Macaca mulatta* (Macaque), *Cebus capucinus* (white-faced sapajou), *Otolemur garnettii* (Northern greater galago), *Mus musculus* (Mouse), *Rattus norvegicus* (Rat), *Equus caballus* (Horse), *Tursiops truncatus* (Dolphin), *Bos taurus* (Cow), *Felis catus* (Cat), *Canis lupus familiaris* (Dog), *Pteropus vampyrus* (Megabat), *Myotis lucifugus* (Micro bat), *Erinaceus europaeus* (Hedgehog), *Echinops telfairi* (lesser hedgehog tenrec), *Monodelphis domestica* (Opossum), *Gallus gallus* (Chicken), *Anolis carolinensis* (Anole lizard), *Latimeria chalumnae* (Coelacanth), *Oryzias latipes* (Medaka), *Gasterosteus aculeatus* (Stickleback), *Tetraodon nigroviridis* (Tetraodon), *Takifugu rubripes* (Fugu), *Danio rerio* (Zebra fish), *Lepisosteus oculatus* (Spotted gar), *Callorhynchus milii* (Elephant shark), *Rhincodon typus* (Whale Shark).

### Sequence analysis

Protein sequences were aligned by using CLUSTAL W through MEGA5 [25]. The phylogenetic tree of *UCHL1* was reconstructed by applying NJ method [55, 56]. Complete deletion option was used for removing gaps and missing data in the protein sequences. Poisson corrected (PC) amino acid distance and uncorrected p-distance of amino acids were used as amino acid substitution models [57]. Due to the similar results obtained with both aforementioned models only NJ tree based on uncorrected p-distance is presented (Fig. 1). ML tree was also constructed by using the Whelan and Goldman (WAG) model of amino acid substitutions [58] (Additional file 1: Figure S1). To ensure the reliability and accuracy of the both NJ and ML trees, topologies bootstrap method was used (at 1000 pseudo replicates), which assigns the bootstrap values to each branch of the tree [59].

ML method and WAG model of amino acid substitution were used to predict ancestral sequences of *UCHL1*. Z-test is executed with MEGA [25] to examine selection constraint within hominoids (human, chimpanzee, gorilla and orangutan), non-hominoids (macaque, marmoset, squirrel monkey and bush baby), non-primate placental mammals (mouse, cat, cow and elephant) and non-mammalian tetrapods (chicken, turtle, frog and coelacanth). Goldman And Yang (GY-94) method (codon based model) implemented in Hyphy program was employed to calculate dN-dS for each of the aforementioned sarcopterygians groups [60].

Domains, motifs and sub-motifs were assigned to human *UCHL1* by ratification from different databases like pfam [28] and MyHit tool [29]. Clustal Omega [61] was employed for multiple sequence alignment to map the putative positions and locations of domains, motifs and sub-motifs on human *UCHL1* and also in orthologous sequences from selected sarcopterygian animals (Fig. 2a). Identified evolutionary substitutions and previously reported human PD and SPG79 causing missense mutations (E7A, S18Y, I93M, R178Q, A216D) were mapped on the human *UCHL1* (Fig. 2a). To estimate the negatively constrained residues of *UCHL1* among sarcopterygians, we employed Single Likelihood Ancestor Counting (SLAC) method through Hyphy which uses global codon model and maximum likelihood to reconstruct the evolutionary history [60]. The impact of all substitutions identified within mammalian history of *UCHL1* were also classified into neutral or radical on the basis of their physicochemical properties, i.e. charge, volume, polarity [62, 63].

### Structural analysis

X-ray structure of human *UCHL1* (2ETL) was retrieved from RCSB Protein Data Bank (PDB) [64]. This X-ray structure was used as a reference in the comparative



structural analysis to evaluate the structural deviations, both in evolutionary and disease perspective. Ancestral protein sequences (Mammalian ancestral, primate's ancestral, simian ancestor and apes/human ancestor) were predicted by ancestral reconstruction technique with wild type UCHL1 structure as a reference to model the ancestral proteins (aforementioned) through homology modeling program MODELLER9 [65]. Best structures were scrutinized on the basis of Discrete Optimized Protein Energy score. For improving the quality of the modeled protein structures, energy minimization protocols were employed through YASARA energy minimization server [66]. For further quality validation of the modeled structures, RAMPAGE [67] and ERRAT [68] were employed (Additional file 1: Figure S6). MuPro was used to investigate the impact of lineage specific substitutions on the modeled ancestral UCHL1 [69]. X-ray structure of human UCHL1 was also used as a reference to model the protein structures of human PD and other neurological disorders causing missense variants of UCHL1 (E7A, S18Y, I93M, R178Q, and A216D) via homology modeling program MODELLER9 [65]. Furthermore, we also predicted the structures of wild-type and disease causing mutant versions of UCHL1 protein through I-TASSER server [70] (Additional file 1: Figure S3) and Robetta server (<https://robetta.bakerlab.org/>) (Additional file 1: Figure S4). Aforementioned protocol is used to minimize, validate and check the quality of PD and other neurological disorder causing mutant models of UCHL1 (Additional file 1: Figure S7). Superimposition of all modeled disease-causing mutant versions of UCHL1 with their wild type version was carried out by Chimera and root mean square deviation (RMSD) values were calculated [71]. For protein-protein interaction analysis of human UCHL1, Cluspro protein-protein docking server [72] was utilized. X-ray structure of interacting partners of UCHL1, i.e. SNCA and PRKIN were obtained from PDB. Interaction between human UCHL1, human SNCA and human PRKIN were examined with the help of Ligplot [73] and PyMol [74].

## Supplementary information

**Supplementary information** accompanies this paper at <https://doi.org/10.1186/s12862-020-01684-7>.

**Additional file 1.** Supplementary Figures.

**Additional file 2.** Supplementary Tables.

**Additional file 3.** Complete list of protein sequences used in this study.

## Abbreviations

UCHL1: Ubiquitin C-Terminal Hydrolase 1; AD: Alzheimer's disease; ML: Maximum Likelihood; NJ: Neighbor-Joining; PC: Poisson corrected; WAG: Whelan and Goldman; RMSD: Root Mean Square Deviation; PD: Parkinson's disease; SLAC: Single Likelihood Ancestor Counting;

PDB: Protein Data Bank; PKC: Protein Kinase C; CK2: Casein Kinase II; UPP: Ubiquitin Proteasome Pathway

## Acknowledgments

The authors thank Yasir Mahmood Abbasi (computer programmer) for technical support.

## Authors' contributions

A.A.A. conceived the project. A.A.A. and Y.B. designed the experiments. M.S.N., R.A. and N.P. performed the experiments. A.A.A., M.S.N., Y.B., R.A., N.P., S.A., I.H. and P.X. analyzed the data. A.A.A., M.S.N., Y.B., and P.X. wrote the paper. All authors have read and approved the final manuscript.

## Funding

This work was supported by National Key Research and Development Program of China [2016Y FE0206600 to Y.B.]; The 13th Five-year Informatization Plan of Chinese Academy of Sciences [XXH13505-05 to Y.B.]; The Professional Association of the Alliance of International Science Organizations [ANSO-PA-2020-07 to Y.B.]; The Open Biodiversity and Health Big Data Program of IUBS [to Y.B.].

## Availability of data and materials

The datasets analyzed during the current study are available in the Ensemble database (<http://www.ensembl.org>), NCBI database (<https://www.ncbi.nlm.nih.gov/>).

## Ethics approval and consent to participate

Not applicable.

## Consent for publication

Not applicable.

## Competing interests

The authors declare that they have no competing interests.

## Author details

<sup>1</sup>National Center for Bioinformatics, Program of Comparative and Evolutionary Genomics, Faculty of Biological Sciences, Quaid-i-Azam University, Islamabad 45320, Pakistan. <sup>2</sup>National Genomics Data Center & CAS Key Laboratory of Genome Sciences and Information, Beijing Institute of Genomics, Chinese Academy of Sciences and China National Center for Bioinformation, Beijing 100101, China. <sup>3</sup>University of Chinese Academy of Sciences, Beijing 100049, China.

Received: 14 January 2020 Accepted: 7 September 2020

Published online: 07 October 2020

## References

- Kumar R, Jangir DK, Verma G, Shekhar S, Hanpude P, Kumar S, et al. S-nitrosylation of UCHL1 induces its structural instability and promotes  $\alpha$ -synuclein aggregation. *Sci Rep*. 2017;7:44558.
- Siddiqui IJ, Pervaiz N, Abbasi AA. The Parkinson disease gene SNCA: evolutionary and structural insights with pathological implication. *Sci Rep*. 2016;6:24475.
- Lee Y-T C, Hsu S-T D. Familial mutations and post-translational modifications of UCHL1 in Parkinson's disease and neurodegenerative disorders. *Curr Protein Pept Sci*. 2017;18(7):733–45.
- De Virgilio A, Greco A, Fabbrini G, Inghilleri M, Rizzo MI, Gallo A, et al. Parkinson's disease: autoimmunity and neuroinflammation. *Autoimmun Rev*. 2016;15(10):1005–11.
- Lunati A, Lesage S, Brice A. The genetic landscape of Parkinson's disease. *Rev Neurol*. 2018;174(9):628.
- Zhang M, Cai F, Zhang S, Zhang S, Song W. Overexpression of ubiquitin carboxyl-terminal hydrolase L1 (UCHL1) delays Alzheimer's progression in vivo. *Sci Rep*. 2014;4:7298.
- Bilguvar K, Tyagi NK, Ozkara C, Tuysuz B, Bakircioglu M, Choi M, et al. Recessive loss of function of the neuronal ubiquitin hydrolase UCHL1 leads to early-onset progressive neurodegeneration. *Proc Natl Acad Sci U S A*. 2013;110(9):3489–94.

8. Nazé P, Vuillaume I, Destée A, Pasquier F, Sablonnière B. Mutation analysis and association studies of the ubiquitin carboxy-terminal hydrolase L1 gene in Huntington's disease. *Neurosci Lett*. 2002;328(1):1–4.
9. Belin AC, Westerlund M, Bergman O, Nissbrandt H, Lind C, Sydow O, et al. S18Y in ubiquitin carboxy-terminal hydrolase L1 (UCH-L1) associated with decreased risk of Parkinson's disease in Sweden. *Parkinsonism Relat Disord*. 2007;13(5):295–8.
10. Leroy E, Boyer R, Auburger G, Leube B, Ulm G, Mezey E, et al. The ubiquitin pathway in Parkinson's disease. *Nature*. 1998;395(6701):451.
11. Rydning SL, Backe PH, Sousa MM, Iqbal Z, Øye A-M, Sheng Y, et al. Novel UCHL1 mutations reveal new insights into ubiquitin processing. *Hum Mol Genet*. 2016;26(6):1031–40.
12. Das C, Hoang QQ, Kreinbring CA, Luchansky SJ, Meray RK, Ray SS, et al. Structural basis for conformational plasticity of the Parkinson's disease-associated ubiquitin hydrolase UCH-L1. *Proc Natl Acad Sci U S A*. 2006;103(12):4675–80.
13. Ragland M, Hutter C, Zabetian C, Edwards K. Association between the ubiquitin carboxyl-terminal esterase L1 gene (UCHL1) S18Y variant and Parkinson's disease: a HuGE review and meta-analysis. *Am J Epidemiol*. 2009;170(11):1344–57.
14. Sasaki H, Yukiue H, Moiriyama S, Kobayashi Y, Nakashima Y, Kaji M, et al. Clinical significance of matrix metalloproteinase-7 and Ets-1 gene expression in patients with lung cancer. *J Surg Res*. 2001;101(2):242–7.
15. Yamazaki T, Hibi K, Takase T, Tezel E, Nakayama H, Kasai Y, et al. PGP9.5 as a marker for invasive colorectal cancer. *Clin Cancer Res*. 2002;8(1):192–5.
16. Kabuta T, Furuta A, Aoki S, Furuta K, Wada K. Aberrant interaction between Parkinson disease-associated mutant UCH-L1 and the lysosomal receptor for chaperone-mediated autophagy. *J Biol Chem*. 2008;283(35):23731–8.
17. Li H, Kiyama H, Osaka H, Kimura I, Nishikawa K, Namikawa K, et al. Ubiquitin carboxy-terminal hydrolase L1 binds to and stabilizes monoubiquitin in neuron. *Hum Mol Genet*. 2003;12(16):1945–58.
18. Nishikawa K, Li H, Kawamura R, Osaka H, Wang Y-L, Hara Y, et al. Alterations of structure and hydrolase activity of parkinsonism-associated human ubiquitin carboxyl-terminal hydrolase L1 variants. *Biochem Biophys Res Commun*. 2003;304(1):176–83.
19. Setsuie R, Wang Y-L, Mochizuki H, Osaka H, Hayakawa H, Ichihara N, et al. Dopaminergic neuronal loss in transgenic mice expressing the Parkinson's disease-associated UCH-L1 I93M mutant. *Neurochem Int*. 2007;50(1):119–29.
20. Setsuie R, Wada K. The functions of UCH-L1 and its relation to neurodegenerative diseases. *Neurochem Int*. 2007;51(2–4):105–11.
21. Cartier AE, Ubhi K, Spencer B, Vazquez-Roque RA, Kosberg KA, Forgeaud L, et al. Differential effects of UCHL1 modulation on alpha-synuclein in PD-like models of alpha-synucleinopathy. *PLoS One*. 2012;7(4):e34713.
22. Mellick G, Silburn P. The ubiquitin carboxy-terminal hydrolase-L1 gene S18Y polymorphism does not confer protection against idiopathic Parkinson's disease. *Neurosci Lett*. 2000;293(2):127–30.
23. Miyake Y, Tanaka K, Fukushima W, Kiyohara C, Sasaki S, Tsuboi Y, et al. UCHL1 S18Y variant is a risk factor for Parkinson's disease in Japan. *BMC Neurol*. 2012;12(1):62.
24. Yousaf A, Sohail Raza M, Ali AA. The evolution of bony vertebrate enhancers at odds with their coding sequence landscape. *Genome Biol Evol*. 2015;7(8):2333–43.
25. Tamura K, Peterson D, Peterson N, Stecher G, Nei M, Kumar S. MEGA5: molecular evolutionary genetics analysis using maximum likelihood, evolutionary distance, and maximum parsimony methods. *Mol Biol Evol*. 2011;28(10):2731–9.
26. Abbasi AA. Molecular evolution of HR, a gene that regulates the postnatal cycle of the hair follicle. *Sci Rep*. 2011;1:32.
27. Abbasi AA, Goode DK, Amir S, Grzeschik K-H. Evolution and functional diversification of the GLI family of transcription factors in vertebrates. *Evol Bioinforma*. 2009;5:S2322.
28. Punta M, Coghill PC, Eberhardt RY, Mistry J, Tate J, Boursnell C, et al. The Pfam protein families database. *Nucleic Acids Res*. 2011;40(D1):D290–301.
29. Pagni M, Ioannidis V, Cerutti L, Zahn-Zabal M, Jongeneel CV, Falquet L. MyHits: a new interactive resource for protein annotation and domain identification. *Nucleic Acids Res*. 2004;32(suppl\_2):W332–5.
30. Bett JS, Ritorto MS, Ewan R, Jaffray EG, Virdee S, Chin JW, et al. Ubiquitin C-terminal hydrolases cleave isopeptide-and peptide-linked ubiquitin from structured proteins but do not edit ubiquitin homopolymers. *Biochem J*. 2015;466(3):489–98.
31. Konya C, Hatanaka Y, Fujiwara Y, Uchida K, Nagai Y, Wada K, et al. Parkinson's disease-associated mutations in  $\alpha$ -synuclein and UCH-L1 inhibit the unconventional secretion of UCH-L1. *Neurochem Int*. 2011;59(2):251–8.
32. Liu Z, Meray RK, Grammatopoulos TN, Fredenburg RA, Cookson MR, Liu Y, et al. Membrane-associated farnesylated UCH-L1 promotes  $\alpha$ -synuclein neurotoxicity and is a therapeutic target for Parkinson's disease. *Proc Natl Acad Sci*. 2009;106(12):4635–40.
33. Ortlund EA, Bridgman JT, Redinbo MR, Thornton JW. Crystal structure of an ancient protein: evolution by conformational epistasis. *Science*. 2007;317(5844):1544–8.
34. Lim K-L, Tan JM. Role of the ubiquitin proteasome system in Parkinson's disease. *BMC Biochem*. 2007;8(1):1–10.
35. Szklarczyk D, Morris JH, Cook H, Kuhn M, Wyder S, Simonovic M, et al. The STRING database in 2017: quality-controlled protein-protein association networks, made broadly accessible. *Nucleic Acids Res*. 2016;1:gw937.
36. Trempe J-F, Sauvé V, Grenier K, Seirafi M, Tang MY, Ménade M, et al. Structure of parkin reveals mechanisms for ubiquitin ligase activation. *Science*. 2013;340(6139):1451–5.
37. Ciechanover A, Kwon YT. Degradation of misfolded proteins in neurodegenerative diseases: therapeutic targets and strategies. *Exp Mol Med*. 2015;47(3):e147.
38. Sulistio YA, Heese K. The ubiquitin-proteasome system and molecular chaperone deregulation in Alzheimer's disease. *Mol Neurobiol*. 2016;53(2):905–31.
39. Huang Q, Figueiredo-Pereira ME. Ubiquitin/proteasome pathway impairment in neurodegeneration: therapeutic implications. *Apoptosis*. 2010;15(11):1292–311.
40. Schwartz AL, Ciechanover A. Targeting proteins for destruction by the ubiquitin system: implications for human pathobiology. *Annu Rev Pharmacol Toxicol*. 2009;49:73–96.
41. Tramutola A, Di Domenico F, Barone E, Perluigi M, Butterfield DA. It is all about (U) biquitin: role of altered ubiquitin-proteasome system and UCHL1 in Alzheimer disease. *Oxidative Med Cell Longev*. 2016;2016:1.
42. Gadhav K, Bolshette N, Ahire A, Pardeshi R, Thakur K, Trandafir C, et al. The ubiquitin proteasomal system: a potential target for the management of Alzheimer's disease. *J Cell Mol Med*. 2016;20(7):1392–407.
43. McNaught KSP, Jenner P. Proteasomal function is impaired in substantia nigra in Parkinson's disease. *Neurosci Lett*. 2001;297(3):191–4.
44. Ma S, Attarwala IY, Xie X-Q. SQSTM1/p62: a potential target for neurodegenerative disease. *ACS Chem Neurosci*. 2019;10(5):2094–114.
45. Kyratzi E, Pavlaki M, Stefanis L. The S18Y polymorphic variant of UCH-L1 confers an antioxidant function to neuronal cells. *Hum Mol Genet*. 2008;17(14):2160–71.
46. Bishop P, Rocca D, Henley JM. Ubiquitin C-terminal hydrolase L1 (UCH-L1): structure, distribution and roles in brain function and dysfunction. *Biochem J*. 2016;473(16):2453–62.
47. Kim H-J, Kim HJ, Jeong J-E, Baek JY, Jeong J, Kim S, et al. N-terminal truncated UCH-L1 prevents Parkinson's disease associated damage. *PLoS One*. 2014;9(6):e99654.
48. Suikowska JI, Rawdon EJ, Millett KC, Onuchic JN, Stasiak A. Conservation of complex knotting and slipknotting patterns in proteins. *Proc Natl Acad Sci U S A*. 2012;109(26):E1715–23.
49. Bishop P, Rubin P, Thomson AR, Rocca D, Henley JM. The ubiquitin C-terminal hydrolase L1 (UCH-L1) C terminus plays a key role in protein stability, but its farnesylation is not required for membrane association in primary neurons. *J Biol Chem*. 2014;289(52):36140–9.
50. Zerbino DR, Achuthan P, Akanni W, Amode MR, Barrell D, Bhai J, et al. Ensembl 2018. *Nucleic Acids Res*. 2017;46(D1):D754–61.
51. Wheeler DL, Barrett T, Benson DA, Bryant SH, Canese K, Chetvernin V, et al. Database resources of the national center for biotechnology information. *Nucleic Acids Res*. 2007;36(suppl\_1):D13–21.
52. Altschul SF, Gish W, Miller W, Myers EW, Lipman DJ. Basic local alignment search tool. *J Mol Biol*. 1990;215(3):403–10.
53. Pervaiz N, Shakeel N, Qasim A, Zehra R, Anwar S, Rana N, et al. Evolutionary history of the human multigene families reveals widespread gene duplications throughout the history of animals. *BMC Evol Biol*. 2019;19(1):128.
54. Seemab S, Pervaiz N, Zehra R, Anwar S, Bao Y, Abbasi AA. Molecular evolutionary and structural analysis of familial exudative vitreoretinopathy associated FZD4 gene. *BMC Evol Biol*. 2019;19(1):72.
55. Saitou N, Nei M. The neighbor-joining method: a new method for reconstructing phylogenetic trees. *Mol Biol Evol*. 1987;4(4):406–25.

56. Russo C. Efficiencies of different statistical tests in supporting a known vertebrate phylogeny. *Mol Biol Evol.* 1997;14(10):1078–80.
57. Tamura K, Nei M, Kumar S. Prospects for inferring very large phylogenies by using the neighbor-joining method. *Proc Natl Acad Sci U S A.* 2004;101(30):11030–5.
58. Whelan S, Goldman N. A general empirical model of protein evolution derived from multiple protein families using a maximum-likelihood approach. *Mol Biol Evol.* 2001;18(5):691–9.
59. Felsenstein J. Confidence limits on phylogenies: an approach using the bootstrap. *Evolution.* 1985;39(4):783–91.
60. Goldman N, Yang Z. A codon-based model of nucleotide substitution for protein-coding DNA sequences. *Mol Biol Evol.* 1994;11(5):725–36.
61. Sievers F, Wilm A, Dineen D, Gibson TJ, Karplus K, Li W, et al. Fast, scalable generation of high-quality protein multiple sequence alignments using Clustal omega. *Mol Syst Biol.* 2011;7(1):539.
62. Grantham R. Amino acid difference formula to help explain protein evolution. *Science.* 1974;185(4154):862–4.
63. Betts MJ, Russell RB. Amino acid properties and consequences of substitutions. *Bioinformatics Genet.* 2003;1:289–316.
64. Berman HM, Westbrook J, Feng Z, Gilliland G, Bhat TN, Weissig H, et al. The protein data Bank. *Nucleic Acids Res.* 2000;28(1):235–42.
65. Webb B, Sali A. Comparative protein structure modeling using MODELLER. *Curr Protoc Bioinformatics.* 2014;47(1):1–5.6.
66. Krieger E, Joo K, Lee J, Lee J, Raman S, Thompson J, et al. Improving physical realism, stereochemistry, and side-chain accuracy in homology modeling: four approaches that performed well in CASP8. *Proteins.* 2009;77(S9):114–22.
67. Lovell SC, Davis IW, Arendall WB III, De Bakker PI, Word JM, Prisant MG, et al. Structure validation by Ca geometry:  $\phi$ ,  $\psi$  and C $\beta$  deviation. *Proteins.* 2003;50(3):437–50.
68. Colovos C, Yeates TO. Verification of protein structures: patterns of nonbonded atomic interactions. *Protein Sci.* 1993;2(9):1511–9.
69. Cheng J, Randall A, Baldi P. Prediction of protein stability changes for single-site mutations using support vector machines. *Proteins.* 2006;62(4):1125–32.
70. Yang J, Zhang Y. I-TASSER server: new development for protein structure and function predictions. *Nucleic Acids Res.* 2015;43(W1):W174–81.
71. Pettersen EF, Goddard TD, Huang CC, Couch GS, Greenblatt DM, Meng EC, et al. UCSF chimera—a visualization system for exploratory research and analysis. *J Comput Chem.* 2004;25(13):1605–12.
72. Comeau SR, Gatchell DW, Vajda S, Camacho CJ. ClusPro: a fully automated algorithm for protein–protein docking. *Nucleic Acids Res.* 2004;32(suppl\_2):W96–9.
73. Wallace AC, Laskowski RA, Thornton JM. LIGPLOT: a program to generate schematic diagrams of protein–ligand interactions. *Protein Eng Des Sel.* 1995;8(2):127–34.
74. DeLano W. The PyMOL molecular graphics system, version 1.3 r1. Schrödinger, LLC, New York; 2010. p. 1–10.

## Publisher's Note

Springer Nature remains neutral with regard to jurisdictional claims in published maps and institutional affiliations.

**Ready to submit your research? Choose BMC and benefit from:**

- fast, convenient online submission
- thorough peer review by experienced researchers in your field
- rapid publication on acceptance
- support for research data, including large and complex data types
- gold Open Access which fosters wider collaboration and increased citations
- maximum visibility for your research: over 100M website views per year

**At BMC, research is always in progress.**

Learn more [biomedcentral.com/submissions](https://biomedcentral.com/submissions)

